CDP-ES- 79-20
Issued 11/27/79
Copy No. X

Distribution on last page.

EXPERIMENTAL STATION
RESEARCH AND DEVELOPMENT DIVISION TECHNICAL REPORT
CHEMICALS, DYES AND PIGMENTS DEPARTMENT
E. I. DU PONT DE NEMOURS & COMPANY

LIGHT SCATTERING AND ABSORPTION BY RUTILE PARTICLES IN WATER, AT WAVELENGTH 254 NANOMETERS, FOR USE IN SIZE ANALYSIS BY SEDIMENTATION FIELD FLOW FRACTIONATION

Work Done By: W. D. Ross

Report Written By: W. D. Ross

Approved By: W. J. Marshall

Patent Situation Approved By: J. W. Heberling, Jr. Date: 11/7/79

Previous Related Reports: None on this specific problem

Project Code: 7053-184086

Type Technical Work: IEB

Period Covered: July 20, 1979 to October 11, 1979

Notebook Nos.: Computer Output Aug. 30, Sept. 5 & 13, 1979

ABSTRACT

The absorption and scattering coefficients of rutile spheres in water for ultraviolet light of wavelength 254 nanometers are presented in graphs and tables.

The technique of sedimentation flow field fractionation has a theoretical potential advantage for analyzing particle size distributions of TiO_2 pigments, compared with sedimentation rate.

INTRODUCTION AND OBJECTIVE

J. J. Kirkland W. W. Yau[1] of the Central Research and Development Department are developing a technique for fractionating dispersions of particles and macromolecules which is called sedimentation flow field fractionation. Among the substances on which they tested the method, they included TiO_2 pigment. Their method of determining the concentration in the effluent stream involves measuring the absorption and scattering of light from a mercury lamp, using the ultraviolet spectrum line at 254 nanometers. To assist this, they asked me to compute the optical properties of the pigment, as a function of particle size.

SUMMARY AND CONCLUSIONS

The absorption and scattering coefficients of rutile spheres in water at wavelength 254 nanometers are presented in graphs and tables.

The technique of sedimentation flow field fractionation depends on sedimentation equilibrium, not sedimentation rate. It has the theoretical potential of analyzing size distributions of TiO_2, not including the larger agglomerates, according to particle mass, without the uncertainties inherent in the sedimentation rate methods which we use. Old calculations are appended which show that the upper limit of size of TiO_2 particle for which it would be useful would be the mass of a sphere of diameter about 0.8 micrometer. The equipment needed to work in this range would be somewhat different from that which Kirkland and Yau are developing.

PROGRAM

The Central Research and Development Department is continuing to develop the method for application to macromolecules. Someone in CD&P should confer with them concerning application to pigments.

PATENT PROTECTION

We have no protection on the method discussed.

FILING ACTION

None is contemplated.

TABLE OF CONTENTS

DISCUSSION

A. Optical Properties

I. Refractive Indices

Cardona and Harbeke[2] have published the complex refractive indices of rutile in the visible and ultraviolet. Cardona kindly sent me full page size copies of the graphs. By measuring these, I found the indices at wavelength 2537 Angstroms as follows:

ordinary: $n - ik = 2.443 - 1.779\ i$
extraordinary: $n - ik = 1.707 - 3.018\ i$

I took the refractive index of water at this wavelength from the Landolt-Bornstein Tables[3]:

$n = 1.375$

II. Computations

The program for computing scattering and absorption by spheres was developed from the formulation of the Debye-Mie theory given by van de Hulst[4] and by Kerker[5]. I made separate computations for the ordinary and extraordinary indices, and averaged the resulting scattering functions as if for a mixture of two kinds of isotropic spheres, with twice as many ordinary as extraordinary. This is not accurate, but should be better than the assumption of a single average index, and is probably fairly good.

Calculations were made for 800 diameters from 1 to 800 nanometers, at increments of 1 nm.

III. Results

Figure 1 is a graph of Q_{sca}, the ratio of scattering cross section to geometrical cross section. The lowest curve is for the ordinary index, the top curve is for the extraordinary index, and the middle curve is for the weighted average.

Figure 2 is a graph of Q_{abs}, the ratio of absorption cross section to geometrical cross section. The curves for the two indices cross at about 60 nm. At smaller sizes, the values for the ordinary index are below those for the extraordinary, and at larger sizes those for the ordinary are above. The weighted average is between.

Figure 3 is a graph of the total scattering coefficient, in units of square meters per gram, calculated by

$$S_t = Q_{sca} \times 1.5/(d \times \rho)$$

where d is diameter in micrometers and ρ is the density of rutile, 2.429 g/cm^3. S_t is larger than the Kubelka-Munk back scattering coefficient.

Figure 4 is a graph of the absorption coefficient, in units of square meters per gram, calculated by

$$K = Q_{abs} \times 1.5/(d \times \rho)$$

This is about half of the Kubelka-Munk diffuse absorption coefficient.

Figure 5 is a graph of $\overline{\cos \theta}$, the average direction cosine of the scattered light. The smallest particles scatter light equally forward and backward. The larger particles scatter chiefly forward. The scattering of particles of ordinary index is more concentrated toward the forward direction than is the scattering of particles of the extraordinary index.

Tables 1, 2, and 3, for respectively the ordinary index, the extraordinary index, and the average values, give these same results at increments of diameter of 25 nanometers. In addition, in the last column, they give the angle of refraction, in degrees, for a ray refracted from the water into the air, if the angle of incidence in the water corresponds to the average cosine in the next to last column. If that ray cannot be refracted into the air, but is totally reflected internally, the angle is listed as 90. This column will help indicate whether much of the scattered light will be collected by the detector. If the listed angle is smaller than 90°, and the detector subtends a much smaller angle than that, and the illuminating beam is smaller yet, then the fraction of the scattered light which is collected by the detector will be on the order of magnitude of the ratio of the solid angle subtended by the detector to the solid angle corresponding to the listed angle. (The solid angle subtended by a circle on a sphere is proportional to (1 - cosine of angular radius of the circle)). On the other hand, if the listed angle is much less than 90°, and the receiver is an integrating sphere, then the receiver may collect most of the scattered light. Light which is trapped by total internal reflection in the water will be mostly absorbed. Much of the scattered light will be trapped in this manner when the listed angle is 90°. For the problem at hand, it appears desirable that the detector subtend a small angle, so that most of the scattered light will be extinguished.

B. Applicability of the Analysis to TiO_2 Pigment

I. Basic Phenomena

The phenomena and calculations which underlie the application of sedimentation field flow fractionation to analysis of particle size of TiO_2 pigments is discussed in the Appendix. This is a copy of part of my section of Edge Moor Monthly Report PTE-M-56-12, November, 1956, pages 11 to 13. The calculations were made for anatase, density 3.84, but the results for rutile, density 4.249, would be only slightly different. The reader should read the Appendix before proceeding to the discussion of it which follows.

The quantity in equation (1) is the diffusion coefficient of the particles, which we will hereinafter call D. (Kirkland and Yau[1] use D for it in their eq. (18), and D_s in their eq. (23).) The scale height, which I called h_o in equations (7), (8), and (9), is what they call ℓ in their eq. (2).

Another interesting relation is found by multiplying my eq. (8) and (10) together and substituting in (1):

$$D = vh_o \qquad (11)$$

(continuing the numbering of equations in sequence from the Appendix to avoid duplication).

II. Significance of Scale Height

The scale height, h_o, depends only on the weight of the particle. Shape does not matter. If the particle is a porous agglomerate or floc, h_o is not affected by the porosity, if the pores fill with water; it depends only on the weight of solid.

III. Uncertainty of Settling Rate

The settling velocity, v, is given by eq. (10) for a solid sphere. The derivation of eq. (10) includes the weight of the particle in the numerator, and the resistance factor, $3\pi\eta d$, in the denominator. It is different for non-spherical particles. A porous sphere would have a diameter greater than that of a solid sphere of the same weight, and so would settle more slowly, and be calculated lighter than it actually is. We have sometimes tried to estimate the likely density of agglomerates for interpreting settling rates. Opposing this, if two or more particles are close together, they settle faster than they would if separated. Therefore a suspension which is not extremely dilute tends to indicate particle sizes which are too large.

IV. Horizontal Flow Channel

Sedimentation field flow fractionation sorts particles according to scale height, h_o. Its simplest embodyment for the TiO_2 pigment would include a horizontal closed flow channel of rectangular cross section, of very low height compared with width horizontally. Water flowing through this will have a velocity distribution which, in a vertical section not too near the sides, will be parabolic, with zero velocity at the boundaries and maximum velocity at mid-height. Particles suspended in the water at low concentration will be carried along at velocities corresponding to their heights. Those so heavy that their h_o is a small fraction of channel depth will move very slowly near the bottom of the channel. Those so light that their h_o is greater than the channel depth will move with an average velocity the same as that of the water.

Kirkland and Yau, in their eq. (5), express the ratio of the average particle velocity to average liquid velocity as a function of the ratio of the scale height to channel depth. Figure 6 is a graph of this relationship but with the horizontal scale being half the channel height divided by the scale height, in the range from 0.10 to 100. We see that for good separation, the height of the channel should be at least four times the scale height of the lightest particles to be separated.

At any instant particles of all weights experience a wide range of velocities, from zero up. But if the particles are in the flow channel for much longer than the time required for them to diffuse from the bottom to the top of their ranges, the average velocity of each particle will tend to become close to the average for its weight class. So, if suspension is injected into the channel for only a short time, followed by clear water, particles will emerge from the channel separated by weight, the lightest first, and the heaviest last.

V. Maximum Size

The classification must fail for particles so heavy that their scale heights are less than their own radii. They essentially roll on the bottom. The larger particles project more into the stream.

From the table on page 13 of the appendix, we see that this limits the largest particle which could be classified to about 0.8 micrometer diameter.

VI. Minimum Size

In our usual pigments, the smallest particles which we need to classify are about 0.10 micrometer diameter. We can ignore anything smaller. From the table we see h_o for this size is 270 micrometers, so according to fig. 6 we would want a channel height about one millimeter.

VII. Time for Diffusion

Kirkland and Yau refer to the height of a theoretical plate, a term taken from the engineering of distillation towers. Their equations (18) and (19) give an estimate of it. From a slightly different point of view we might refer analogously to a unit transfer time. After some manipulation of their equations, and introduction of our eq. (11), we can identify this with the time required for the smallest particle to be separated to settle the distance $4h_o$. From the table in the appendix, $4h_o/v$ is 13,500 seconds, or 3.75 hours. Because good separation requires a large number of unit transfer times, this obviously is inconveniently slow.

VIII. Centrifugal Field

Therefore we would need to use a centrifuge, as they do. But we would need much weaker centrifugal fields than they use for most of the materials in which they are interested. For example, a centrifugal field of 10 gravities would decrease h_o by a factor of 10, increase settling rate v by a factor of 10, decrease unit transfer time by a factor of 100. Whereas gravity is a significant fraction of such a centrifugal field, the flow channel should be built on a cone perpendicular to the resultant of the centrifugal field and gravity. If the channel were vertical, as soon as the centrifugal field would concentrate the particles near the outer wall, the entire suspension near the outer wall would flow downward, relatively rapidly, and would not classify in a layer as intended. Perhaps this is not a problem with samples which require much higher centrifugal fields.

But a centrifugal field of 10 gravities would restrict the upper limit of size which could be classified to around 0.45 micrometer. Therefore we would want both a horizontal channel and a centrifuge operating at a single designed speed.

The discussion of unit transfer time might leave the impression that the channel might be very short if the flow rate is low enough. Longitudinal diffusion will fix the lower limit of the "height of a theoretical plate" at some small multiple of h_o, perhaps $2h_o$.

IX. Resolution Desired

In our analyses of single crystal size, the coefficient of variation is around 0.3 (= standard deviation/mean). For an analysis to be useful, it should have much better resolution than this. Also, carbon black undertone is very sensitive to mean crystal size, so we would like the median size determined within a few percent.

WDR/kkg

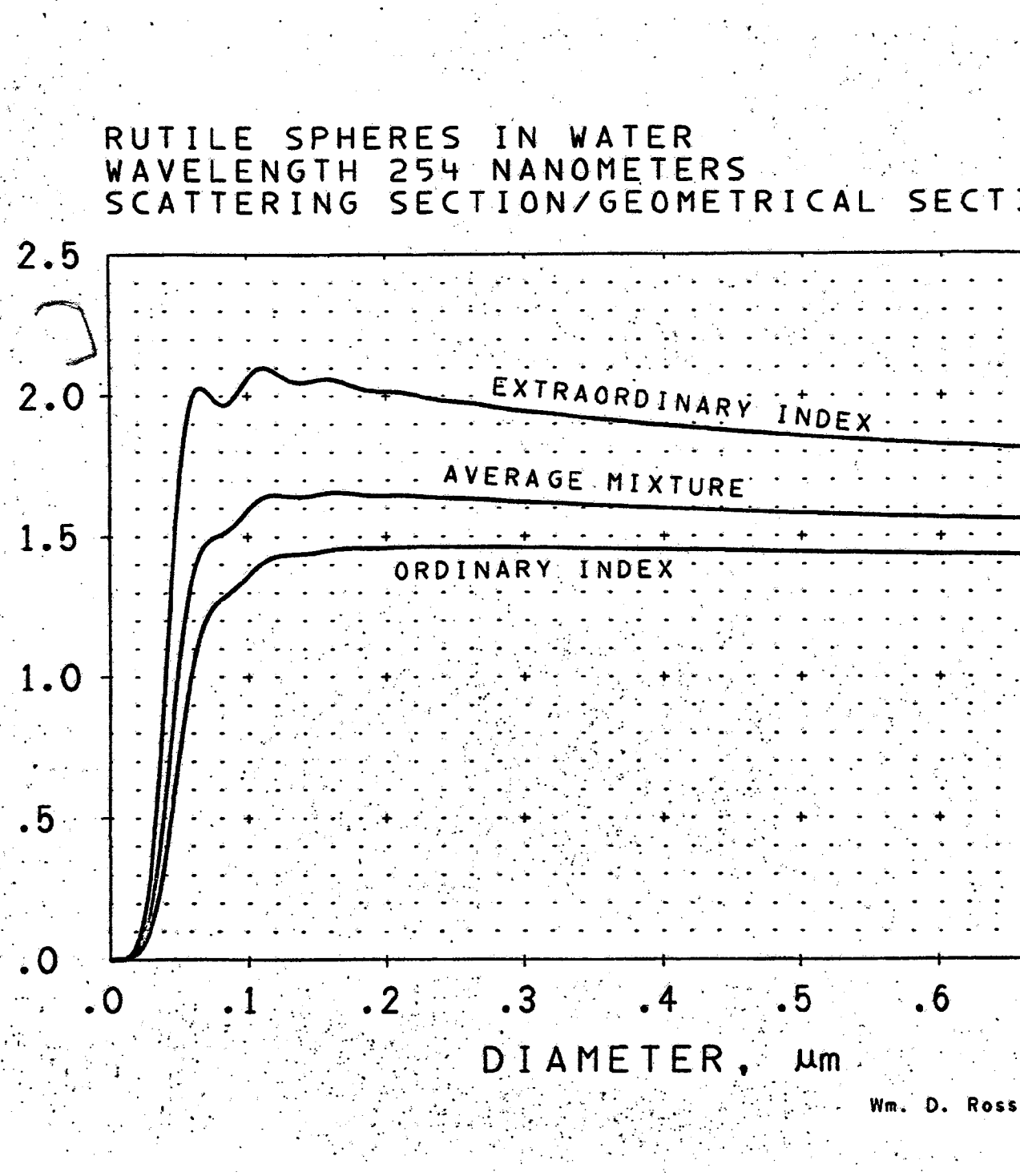

Figure 2

RUTILE SPHERES IN WATER
WAVELENGTH 254 NANOMETERS
ABSORPTION SECTION/GEOMETRICAL SECTION

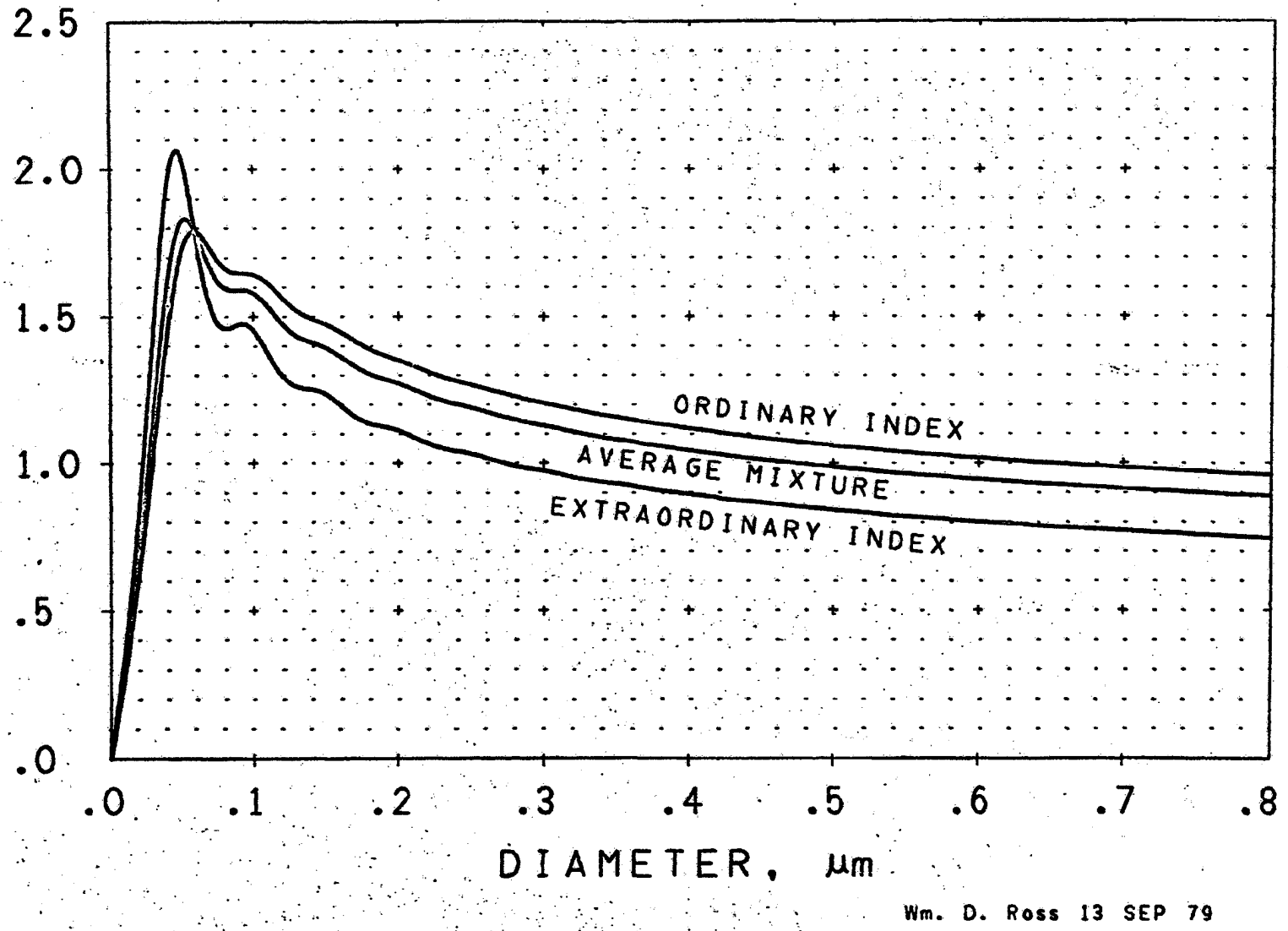

Wm. D. Ross 13 SEP 79

Figure 3

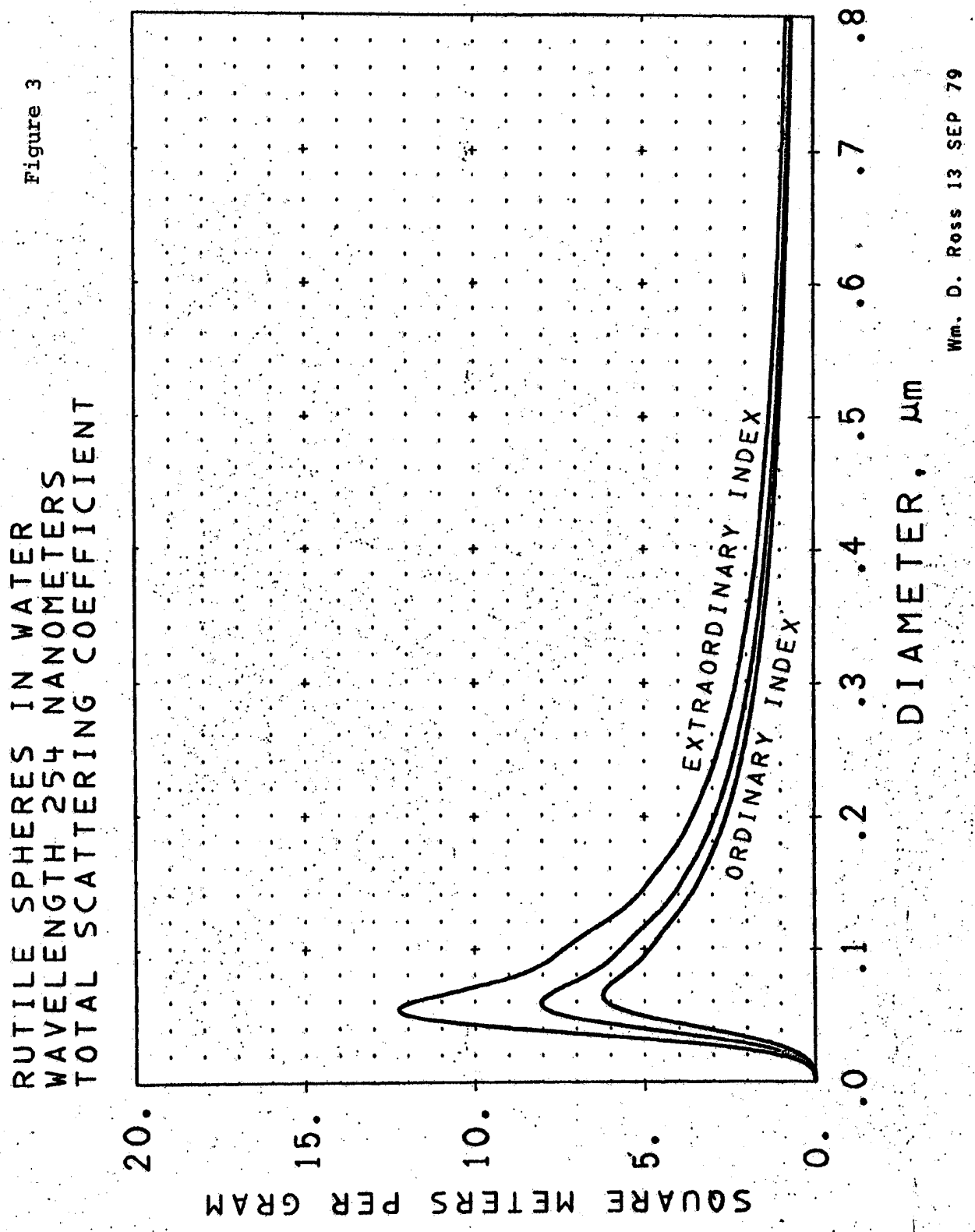

Figure 4

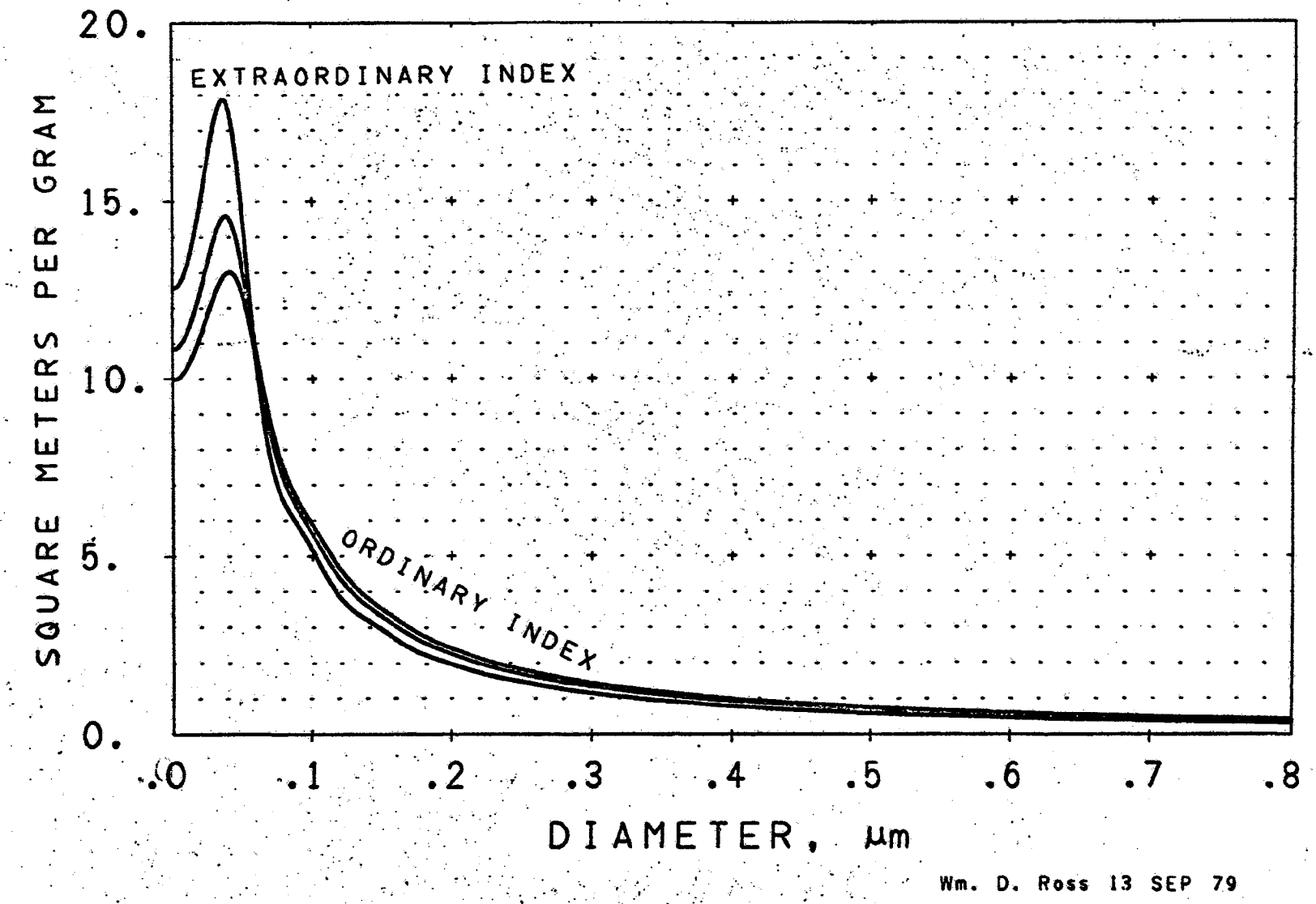

CDP-ES-79-20

Figure 5

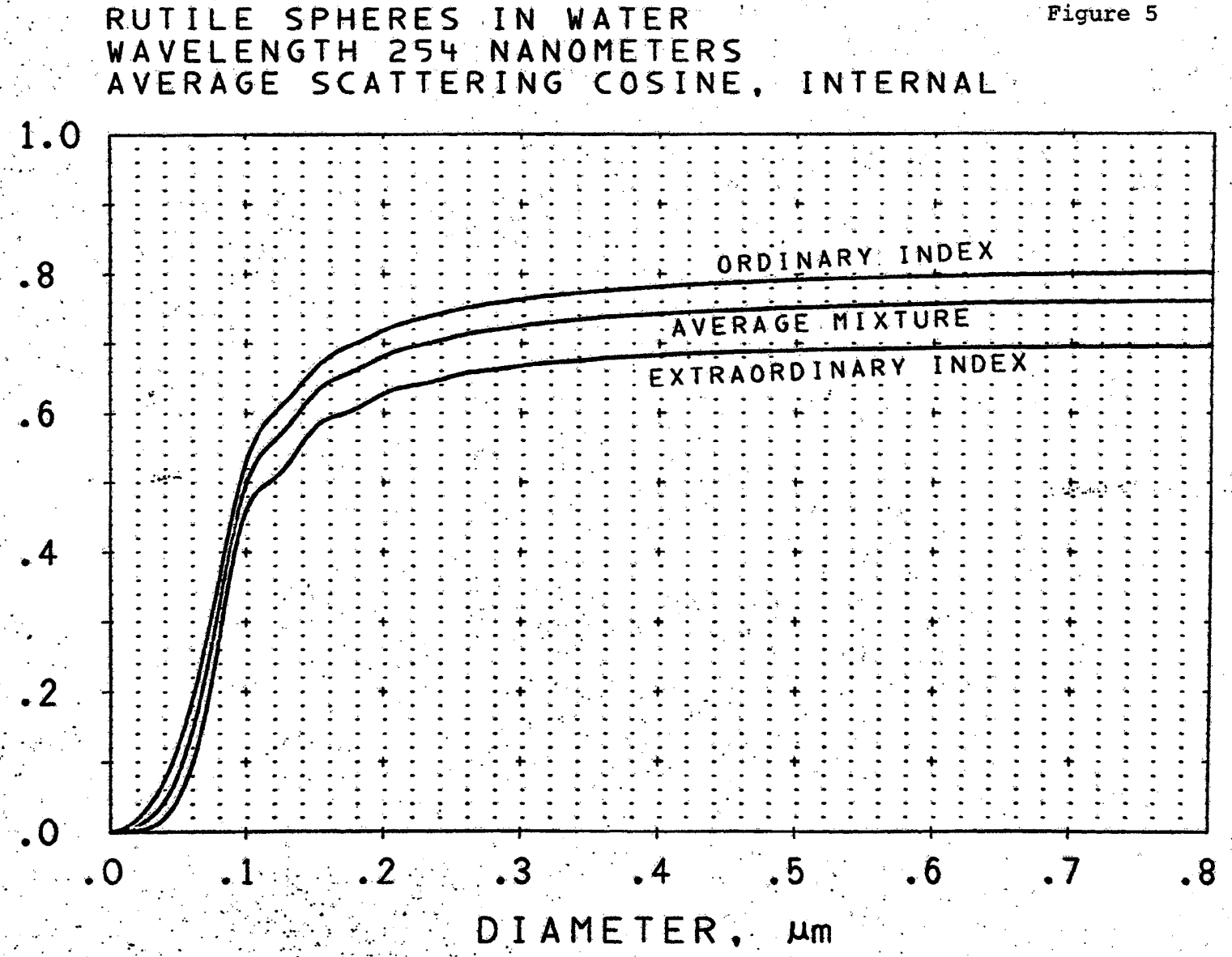

CDP-ES-79-20

KEUFFEL & ESSER CO.

Figure 6

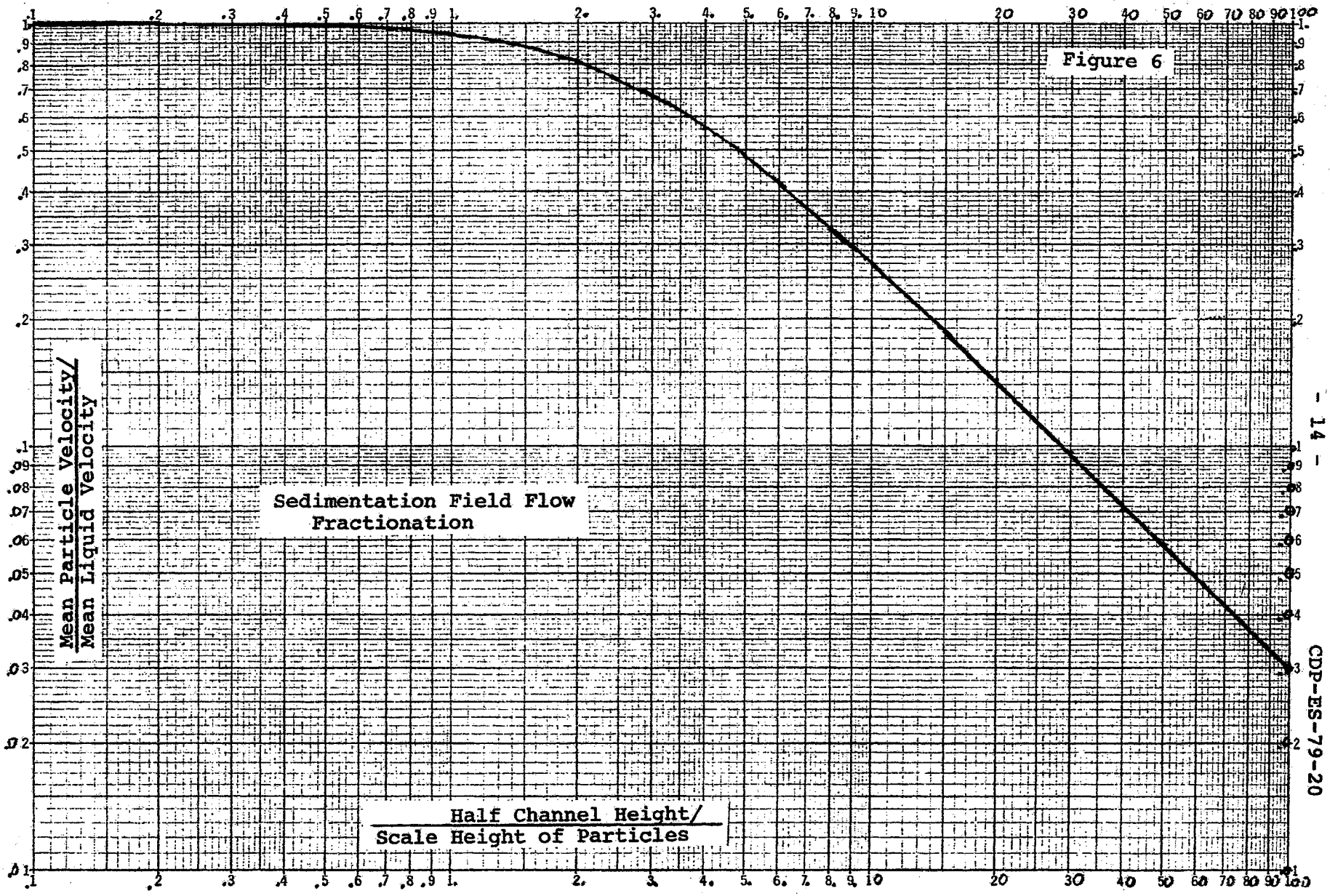

Wm. D. Ross 10/10/79

ROSS MIE DATE 091379

Table 1

MIE THEORY WM. D. ROSS 13 SEP 79

RUTILE SPHERES IN WATER

SPHERES OF REFRACTIVE INDEX 2.443-1.779 I,
IN A MEDIUM OF REFRACTIVE INDEX 1.375, AT WAVELENGTH .254 MICROMETER, DENSITY = 4.249

DIAMETER MICRONS	QABS	QSCA	ABSORPTION SQ. M./G.	SCATTERING SQ. M./G.	AVE. COSINE	AVE. ANGLE IN AIR
.025	.840	.602-01	11.9	.850	.0293	90.
.050	1.74	.730	12.3	5.15	.1245	90.
.075	1.68	1.25	7.92	5.89	.3178	90.
.100	1.64	1.36	5.79	4.81	.5359	90.
.125	1.53	1.43	4.33	4.05	.6122	90.
.150	1.47	1.44	3.46	3.40	.6666	90.
.175	1.40	1.46	2.82	2.94	.6975	80.
.200	1.35	1.46	2.38	2.58	.7200	73.
.225	1.30	1.46	2.04	2.29	.7359	69.
.250	1.26	1.46	1.79	2.06	.7477	66.
.275	1.23	1.46	1.58	1.88	.7570	64.
.300	1.20	1.46	1.41	1.72	.7641	63.
.325	1.18	1.46	1.28	1.58	.7700	61.
.350	1.15	1.46	1.16	1.47	.7747	60.
.375	1.13	1.45	1.07	1.37	.7787	60.
.400	1.12	1.45	.985	1.28	.7820	59.
.425	1.10	1.45	.913	1.20	.7849	58.
.450	1.08	1.45	.851	1.14	.7873	58.
.475	1.07	1.44	.796	1.07	.7894	58.
.500	1.06	1.44	.747	1.02	.7912	57.
.525	1.05	1.44	.704	.969	.7928	57.
.550	1.04	1.44	.665	.923	.7942	57.
.575	1.03	1.44	.630	.882	.7955	56.
.600	1.02	1.43	.598	.844	.7966	56.
.625	1.01	1.43	.569	.809	.7976	56.
.650	.999	1.43	.543	.777	.7985	56.
.675	.992	1.43	.519	.747	.7993	56.
.700	.984	1.43	.497	.720	.8001	56.
.725	.978	1.43	.476	.694	.8007	55.
.750	.971	1.42	.457	.670	.8013	55.
.775	.965	1.42	.440	.648	.8019	55.
.800	.959	1.42	.423	.627	.8024	55.
EXTREMES	1.79	1.46	13.0	6.22	.0000	

ROSS MIE DATE 091379

Table 2

MIE THEORY WM. D. ROSS 13 SEP 79

RUTILE SPHERES IN WATER

SPHERES OF REFRACTIVE INDEX 1.707-3.018 I,
IN A MEDIUM OF REFRACTIVE INDEX 1.375, AT WAVELENGTH .254 MICROMETER. DENSITY = 4.249

DIAMETER MICRONS	QABS	QSCA	ABSORPTION SQ. M./G.	SCATTERING SQ. M./G.	AVE. COSINE	AVE. ANGLE IN AIR
.025	1.15	.159	16.3	2.25	.0031	90.
.050	2.01	1.70	14.2	12.0	.0494	90.
.075	1.47	1.96	6.92	9.34	.2271	90.
.100	1.44	2.07	5.10	7.31	.4657	90.
.125	1.27	2.06	3.58	5.83	.5169	90.
.150	1.23	2.06	2.89	4.84	.5815	90.
.175	1.14	2.03	2.30	4.10	.6033	90.
.200	1.11	2.02	1.96	3.56	.6293	90.
.225	1.06	2.00	1.66	3.13	.6412	90.
.250	1.03	1.98	1.45	2.79	.6539	90.
.275	.994	1.96	1.28	2.52	.6612	90.
.300	.972	1.94	1.14	2.29	.6681	90.
.325	.946	1.93	1.03	2.10	.6730	90.
.350	.928	1.92	.936	1.93	.6771	90.
.375	.908	1.90	.855	1.79	.6805	90.
.400	.893	1.89	.788	1.67	.6830	90.
.425	.877	1.88	.729	1.56	.6854	90.
.450	.864	1.87	.678	1.47	.6870	88.
.475	.851	1.86	.633	1.38	.6887	85.
.500	.840	1.85	.593	1.31	.6899	85.
.525	.829	1.85	.557	1.24	.6911	84.
.550	.819	1.84	.525	1.18	.6919	83.
.575	.809	1.83	.497	1.12	.6927	83.
.600	.800	1.82	.471	1.07	.6933	82.
.625	.792	1.82	.448	1.03	.6939	82.
.650	.784	1.81	.426	.984	.6943	82.
.675	.777	1.81	.406	.945	.6947	81.
.700	.770	1.80	.388	.908	.6950	81.
.725	.763	1.80	.372	.874	.6953	81.
.750	.757	1.79	.356	.843	.6955	81.
.775	.751	1.79	.342	.813	.6957	81.
.800	.745	1.78	.329	.786	.6959	81.
EXTREMES	2.06	2.10	17.9	12.3	.0000	

ROSS MIE DATE 091379

Table 3

MIE THEORY WM. D. ROSS 13 SEP 79

RUTILE SPHERES IN WATER

SPHERES OF REFRACTIVE INDEX 2.443-1.779 I, 1.707-3.018 I,
APPROXIMATED AS A MIXTURE OF SPHERES OF THE TWO INDICES IN PROPORTION 2/1
IN A MEDIUM OF REFRACTIVE INDEX 1.375, AT WAVELENGTH .254 MICROMETER, DENSITY = 4.249

DIAMETER MICRONS	QABS	QSCA	ABSORPTION SQ. M./G.	SCATTERING SQ. M./G.	AVE. COSINE	AVE. ANGLE IN AIR
.025	.945	.931-01	13.3	1.32	.0144	90.
.050	1.83	1.05	12.9	7.43	.0841	90.
.075	1.61	1.50	7.59	7.04	.2777	90.
.100	1.57	1.60	5.56	5.64	.5056	90.
.125	1.44	1.64	4.08	4.64	.5723	90.
.150	1.39	1.65	3.27	3.88	.6312	90.
.175	1.31	1.65	2.65	3.33	.6588	90.
.200	1.27	1.64	2.24	2.90	.6829	90.
.225	1.22	1.64	1.91	2.57	.6975	80.
.250	1.19	1.63	1.68	2.31	.7098	76.
.275	1.15	1.63	1.48	2.09	.7186	73.
.300	1.13	1.62	1.32	1.91	.7257	71.
.325	1.10	1.62	1.19	1.75	.7314	70.
.350	1.08	1.61	1.09	1.62	.7359	69.
.375	1.06	1.60	.997	1.51	.7398	68.
.400	1.04	1.60	.919	1.41	.7429	67.
.425	1.03	1.59	.852	1.32	.7457	66.
.450	1.01	1.59	.793	1.25	.7479	66.
.475	.998	1.58	.741	1.18	.7499	65.
.500	.985	1.58	.696	1.12	.7516	65.
.525	.974	1.58	.655	1.06	.7531	65.
.550	.963	1.57	.618	1.01	.7543	65.
.575	.954	1.57	.585	.963	.7555	64.
.600	.944	1.56	.556	.921	.7565	64.
.625	.936	1.56	.529	.882	.7574	64.
.650	.928	1.56	.504	.846	.7581	64.
.675	.920	1.55	.481	.813	.7588	64.
.700	.913	1.55	.460	.783	.7594	63.
.725	.906	1.55	.441	.754	.7600	63.
.750	.900	1.55	.424	.728	.7605	63.
.775	.894	1.54	.407	.703	.7610	63.
.800	.888	1.54	.392	.680	.7614	63.
EXTREMES	1.83	1.65	14.6	8.04	.0000	

LAST FRAME WRITTEN WAS 7

THE NAME OF YOUR SINDUP FILE IS:
583450*790913-40877,F33///5000

@FIN

CDP-ES+79-20

REFERENCES

1. J. J. Kirkland and W. W. Yau, "Experimental Aspects of Sedimentation Field Flow Fractionation (SFFF)", CRD-79-19 (1979).

2. M. Cardona and G. Harbeke, "Optical Properties and Band Structure of Wurtzite-Type Crystals and Rutile", Phys. Rev. 137, A1467 (1965).

3. Landolt-Bornstein Tabellen. 6 Auflage. II Band. 8 Teil. Optische Konstanten. 5-562.

4. H. C. van de Hulst, "Light Scattering by Small Particles", Wiley, 1957.

5. M. Kerker, "The Scattering of Light and Other Electromagnetic Radiation", Academic Press, 1959.

APPENDIX

MICROSCOPIC STUDY OF PIGMENT DISPERSIONS - Wm. D. Ross

An attachment which we have recently acquired for the microscope is a vertical illuminator with immersion objective. This has proved particularly satisfactory for studying the state of dispersion of a suspension of TiO_2 particles.

When a dispersion of TiO_2 in water is examined, all the particles are in Brownian motion (except for any which adhere to either the microscope slide or the cover glass). But particles a micron and larger in diameter seem to roll and slide on or near the surface of the microscope slide, whereas particles a quarter micron in diameter and smaller move up and down in the depth of the water between the slide and the cover glass. Thus the larger particles can be kept in focus in one plane.

Standard equations of colloid theory have been applied to the behaviour of these dispersions of TiO_2 in water:

Brownian Motion

If particles of diameter d are examined for intervals of t seconds, and the distances travelled during these intervals measured, the average distance travelled along one direction, $\bar{x}$, is given by

$$\frac{\bar{x}^2}{2t} = \frac{kT}{3\pi\eta d} \qquad (1)$$

where k is the Boltzmann constant, and η the viscosity, T is the absolute temperature.

Putting in the proper constants for TiO_2 in water at room temperature, and measuring diameter and distance in microns,

$$\frac{\bar{x}^2}{t} = \frac{0.87}{d} \quad ; \quad \frac{\bar{x}}{\sqrt{t}} = \frac{0.93}{\sqrt{d}} \qquad (2)$$

For very small intervals of time, this equation will not hold, because the average component instantaneous of velocity in the x direction, for which we will write u, is limited:

$$mu^2 = kT \qquad (3)$$

$$m = \text{mass of particle} = \frac{\pi d^3 \rho}{6}$$

$$\rho = \text{density of particle}$$

MICROSCOPIC STUDY OF PIGMENT DISPERSIONS (Con't.)

Again measuring d in microns and u in microns per second,

$$u = \frac{1400}{\sqrt{d^3}} \qquad (4)$$

The equation (2) will be valid for times of observation exceeding

$$t = \frac{\bar{x}^2}{tu^2} = 4.5 \cdot 10^{-7} \ d^2 \text{ second}, \qquad (5)$$

which is too short to measure. During this time the particle would travel what might be considered a mean free path distance,

$$\frac{\bar{x}^2}{tu} = \frac{\sqrt{d}}{1600} \qquad (6)$$

Sedimentation Equilibrium

Where the particles are dilute enough not to be packed together, the concentration of particles of any selected size decreases as height increases, according to

$$\ln \frac{c_1}{c_2} = \frac{h}{h_o} \qquad (7)$$

where c_1 = concentration at lower level

c_2 = concentration at higher level

h = distance between levels (8)

In water,

$$h_o = \frac{6kT}{\pi d^3(\rho - 1)g}$$

ρ = density of TiO_2, grams/cm^3

g = acceleration of gravity

Putting in the proper constants, and measuring dimensions in microns,

$$h_o = \frac{0.268}{d^3} \qquad (9)$$

MICROXCOPIC STUDY OF PIGMENT DISPERSIONS (Con't.)

Sedimentation Rate

The sedimentation equilibrium will be achieved only after sufficient time has elapsed. The settling velocity, according to Stokes' Law is

$$v = \frac{d^2(\rho - 1)g}{18\eta} \qquad (10)$$

The accompanying table gives the results of the foregoing three type of calculations for the range of particle size in which we are interested.

A few observations showed that the thickness of the film of slurry under the cover glass ranges up to 50 microns.

BROWNIAN MOTION, SEDIMENTATION EQUILIBRIUM, AND SEDIMENTATION VELOCITY OF TiO_2 IN WATER

Dimensions in microns; times in seconds

d	(2) $\frac{\bar{x}}{\sqrt{t}}$	(9) h_o	(10) v
1	.9	.3	1.6
.8	1.0	.5	1.0
.6	1.2	1.2	.6
.5	1.3	2.1	.4
.4	1.5	4	.26
.3	1.7	10	.15
.25	1.9	17	.10
.2	2.1	33	.06
.15	2.4	80	.04
.1	3.	270	.02

INDEXING TERMS

Ultraviolet

Light Scattering

Light Absorption

Rutile

TiO_2 Pigment

Size Analysis

Sedimentation

Flow Fractionation

DISTRIBUTION

1. W. D. Ross
2. K. K. Bhatia
3. W. J. Marshall, EM
4. H. B. Clark, W
5. R. A. Darby/A. S. Bjornson/L. T. Frick/J. G. Ishikawa
6. E. C. Broge/M. A. Toomey/J. A. Blumberg
7. J. M. Hustler
8. L. N. Fisher/G. A. Hapka
9-10. Central Report Index
11-14. L. A. Wierzbowski, EM
15. J. J. Kirkland, CR&DD
16. W. W. Yau, CR&DD
17. K. L. Uhland, EM
18. R. W. Hess, EM
19. J. H. Braun
20. H. R. Linton, EM
21. S. V. R. Mastrangelo, EM
22. H. W. Jacobson
23. A. Allen, EM
24. P. G. Schmidt
25. L. A. Monson
26. A. Baidins
27. R. J. Bruehlman, EM
28. J. H. Boughton
29. D. P. Fields, EM
30. H. H. Glaeser
21. P. G. Reis, EM
32. G. D. Gemmell
33. C. R. Buchanan, EM
34. G. E. Lynskey, JV
35. D. U. Gwost, JV
36. M. R. Baloga, JV
37. D. A. Nelson, DeLisle
38. C. M. Paulson, E357
39. R. Davies, L13 W15
40. N. C. Scrivner, L13 W51
41. J. G. Dickinson, Ch. R.
42. W. J. Lawrence, Antioch
43-47. Author's copies